ISBN: 978-3-95450-208-0 doi:10.18429/JACoW-IPAC2019-WEPRB025

HIGH DENSITY MAPPING FOR SUPERCONDUCTING CAVITIES*

H. Tongu, Y. Iwashita#, Kyoto ICR, Uji, Kyoto, Japan
Y. Fuwa, J-PARC center, JAEA, Tokai, Ibaraki, Japan
H. Hayano, KEK, Tsukuba, Ibaraki, Japan
R.L. Geng, JLAB, Newport News, VA 23606, U.S.A.

Abstract

High density mapping system for superconducting cavities are under development. Testing on the stiffener X-ray mapping system at JLAB showed consistent results in comparison with simultaneously taken GM tube or ion chamber output signals. The system provides better visibility as shown by data briefly reported here. In addition to the temperature and the X-ray mapping, a sensitive magnetic field mapping system with high spatial density is also under development. The magnetic field sensor is AF755B, whose operations at cryogenic temperatures are already reported by other group. Our development status using the magnetic field sensor will be reported.

INTRODUCTION

In order to keep or raise the performance of superconducting cavities, inspection systems take important role during the fabrication process. We have been developing high density mapping systems for superconducting cavities. XT-map system is a combined mapping system of temperature mapping system and X-ray mapping system with high density [1] (see Fig. 1). The key technologies are the use of the flexible print circuit and multiplexing system for the huge number of analogue signals from the sensors, which eases the installation hence the required number of wires can be significantly reduced.

The sX-map, stiffener X-ray mapping system, is designed to place similar detector strips under the cavity stiffener rings, allowing installation without using special jigs, etc. It can map X-rays in vicinity of the iris area of a cavity with 32 point azimuthal resolution in one sensor strip (see Fig. 2). Ten sensor strips are installed on a SC cavity at JLAB and mapping of the X-rays from the field emission under a vertical test is carried out. The results are briefly reported in the next section.

In addition to the temperature and the X-ray mapping system, sensitive magnetic field mapping system is also under development. The magnetic field sensor is AF755B, whose operations at cryogenic temperatures are already reported by other group [2]. Our development status using the magnetic field sensor is also reported in the following section.

TEST RESULTS OF SX-MAP

The sX-map system was installed on the LSF5-1 cavity (see Fig. 3 left). While the cell shape and the configuration of the stiffener ring are slightly different from those of a Tesla cavity, four strips could be installed under the rings near four irises between adjacent cells. One sensor strip is installed on each flange: top and bottom. Two strips are installed at the upper beam tube area and one at the lower beam tube (see Fig. 3 right).

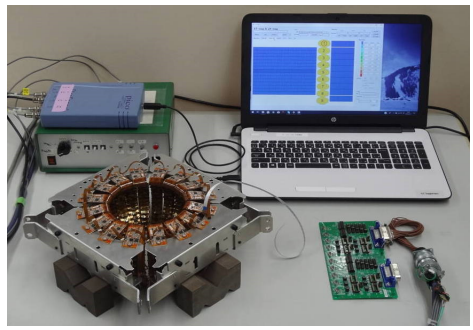

Figure 1: XT-map unit for a cell.

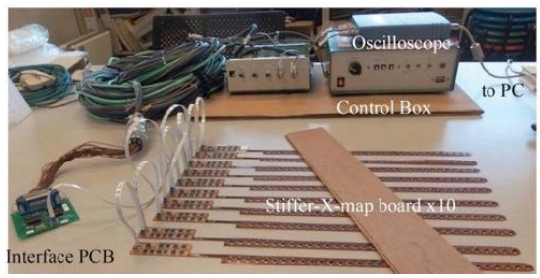

Figure 2: sX-map system with ten strips.

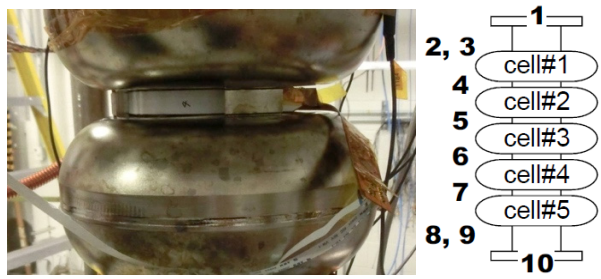

Figure 3: sX-map strip installed to cavity LSF5-1 (left). The ten strip locations are also illustrated (right).

Because of a turbo pump loss subsequent to power failure accident and the foreline scroll pump not working right at the time, the cavity vacuum was compromised while it was fully immersed in 4K liquid helium bath, large quantity of air (up to 61 g in weight) entered into the cavity from the bottom beam tube. Subsequently the cavity showed lots of field emission starting at a rather low gradient. X-ray distributions were mapped under this unintended surface-contaminated condition. Because the current from the sensors are integrated, while the signals are scanned by the analog multiplexor, the sensitivity of

* Work supported by US-Japan collaboration.
# iwashita@kyticr.kuicr.kyoto-u.ac.jp

ISBN: 978-3-95450-208-0 doi:10.18429/JACoW-IPAC2019-WEPRB025

the mapping system can be raised by slowing down the clock speed. Clock periods of 10, 20, 50 and 900 μs are used this time.

Besides the standard JLAB ion chamber counter (IC) permanently mounted at each vertical test Dewar, one GM tube, identical to those used at JLAB for cryomodule acceptance testing, was placed on the top plate of the insert hosting cavity LSF5-1. Both the GM tube and the ion chamber are located within the Dewar radiation shield. We recorded their output signals during the cavity test and these values are compared with the output vectors from the sX-map system by taking norms. Figure 4 shows output signals described above. While the GM tube lost its sensitivity around 5.5 MV/m, the IC kept its sensitivity down to about 4.5 MV/m and faded into noise. Our sX-map system seemed to detect X-rays even at around 4.2 MV/m.

Figure 5 shows typical mapping results from low electric field gradient to high gradient for π-mode excitation in cavity. Each rectangular with mosaic pattern denotes the X-ray map for the given gradient, where each elemental colored box denotes a local sensor signal (warm color, red indicating higher X-ray detection). The mosaic pattern is consisted of 10 belts as indicated by numbers along vertical axis, each for a strip (the same number as in Fig. 3). Each belt is consisted of 32 blocks, each for a sensor in the azimuthal direction. Electric field gradients, numerical values of two external sensors outputs, clock periods and output signal ranges are also shown.

While no signals are shown at 4.05 MV/m (Fig. 5 top), a radiation spot appears around left upper middle area at 4.45 MV/m (Fig. 5 second top) and grew as gradient increases. At 5.16 MV/m, other spots appeared mostly at top and bottom flanges. Distributions were visible even at high radiation level.

Other pass-band modes were also excited and the mapping results are shown in Fig. 6. This allows non-uniform field distribution among individual cells (numbered as 1, 2, 3, 4, 5 from top). The gradient levels shown in the figure corresponds to the gradient in the end cells (cell 1&5). For any mode, gradient in other cells can be found by using the scaling factors given in Table 1. For example, for 4/5- mode shown in Fig. 6(b), gradient in cell 2&4 is $7.98 \times 0.6108 = 4.87$ MV/m; for 3/5-π mode in Fig. 6(c), gradient in cell 3 is 4.72x1.2638 = 5.97 MV/m. While there were not much variations observed when the gradient changed, these distributions should be useful by combining trajectory analysis of electrons emitted from field emission source locations which in turn permits to pin-point field emitters.

Figure 7 shows field pattern for these passband modes. For π-mode, all cells are equally excited with the same electric field. The X-ray map for this mode taken at 5.26 MV/m as shown in Fig. 6(a) breaks the mirror symmetry over the equatorial plane of the center cell with larger signals at strip 7 (just above the bottom cell, cell#5) as compared to that at strip 4 (just below the top cell, cell#1). This indicates presence of source field emitters in the bottom cell. In addition, the azimuthal non-uniformity

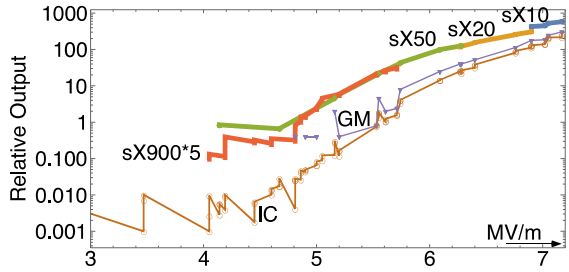

Figure 4: Relative outputs of sX-map, GM tube and ion chamber are shown. Numbers after "sX" denote clock periods in μs.

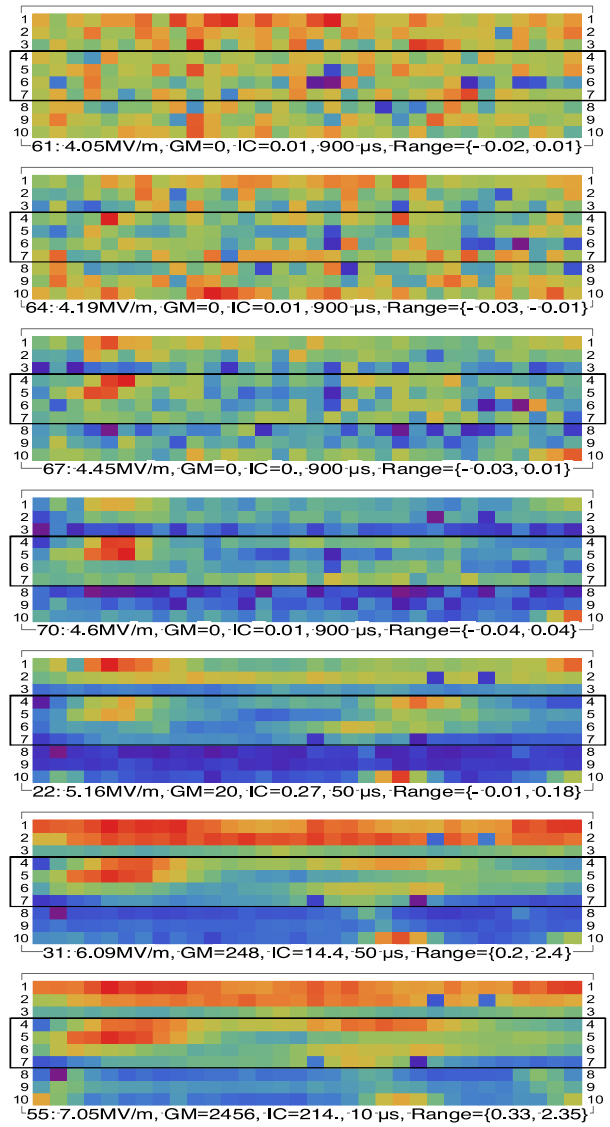

Figure 5: Mapping results for π-mode. 32 sensors are shown horizontally. Ten strips are aligned downwards: indices at both sides. The iris positions (4~7) are boxed.

Table 1: Scaling Factor for Pass-band Mode

Modes	f (GHz)	E_4/E_5	E_3/E_5	Epk/√U (MV/m)	Hpk/√U (mT)
π	1.3000	0.994	0.9933	8.07	11.83
4π/5	1.2985	0.6108	0.0014	10.55	15.85
3π/5	1.2944	0.4239	1.2638	10.96	16.82
2π/5	1.2893	1.6949	0.0029	10.37	16.23
π/5	1.2852	2.7391	3.4087	10.36	16.97

ISBN: 978-3-95450-208-0 doi:10.18429/JACoW-IPAC2019-WEPRB025

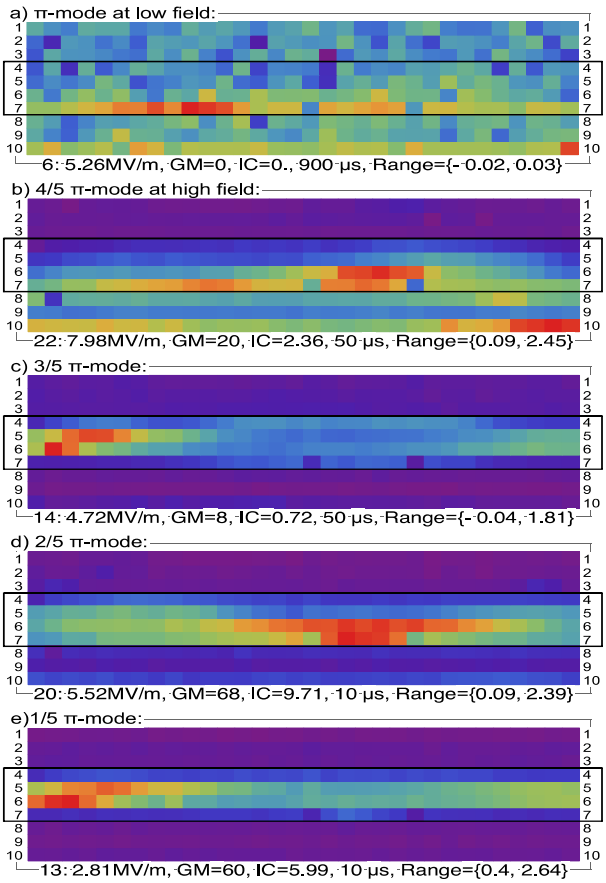

Figure 6: Results for π-, 4/5π-, 3/5π-, 2/5π-, and 1/5π-mode. The naming of the modes is SRF specific.

for signal at strip 7 suggests that source field emitters are distributed around the cell surface with no-uniform concentration. Inspection of X-ray maps shown in Fig. 6(b), (c), (d) for 4/5-π, 3/5-π, and 2/5-π mode reveals similar broken mirror symmetry and they suggest consistently the presence of source field emitters are in the lower cells (Cell#5, Cell#4). Azimuthal non-uniformity suggests distributed nature of field emitters around different cells. In summary, the X-ray mapping system reveals asymmetric cell to cell distribution suggesting presence of field emitters in lower cells (Cell #5, #4, and #3). This is consistent with the fact that large amount of air entered into the cavity from the bottom cell.

SYSTEM OF B-MAP

A schematic block diagram of our B-map system is shown in Fig. 8. Outputs from AFF755B sensor bridges are multiplexed and fed to a differential amplifier. The control block generates multiplexor address and the flipping coil pulse after one sequential scan. Then four sensor system requires eight clocks for full scan. The whole part shown in Fig. 8 will be operated at the cryogenic temperature. We use NJU77552 CMOS amplifier, which can operate at the cryogenic temperature with higher power supply voltage [3]. The measured sensitivity at the room temperature is about 0.4 V/G. This system will be tested at cryogenic temperature in near future.

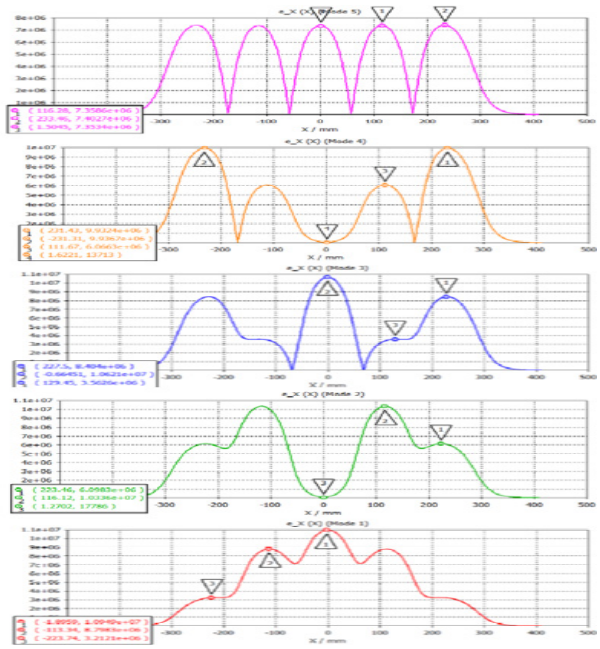

Figure 7: Electric field pattern for passband modes. Note mirror symmetry for cell pair 1&5 and 2&4. (calculation by Gunn Park)

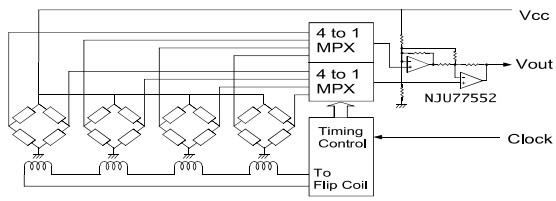

Figure 8: Schematic block diagram of B-map system.

SUMMARY

The sX-map system even with the rather cheap IR sensors seems to have high sensitivity owing to the configuration of sensors being located very close to the cavity wall. The number of wires can be as small as eight, which will reduce the handling, wiring and heat load cost. The XT-map system is under development and waiting for fabrication of one more prototype. The first prototype of B-map system is waiting for an opportunity of test at the cryogenic temperature.

REFERENCES

[1] H. Tongu *et al.*, "Development of High Sensitive X-Ray Mapping for SC Cavities", in *Proc. 8th Int. Particle Accelerator Conf. (IPAC'17)*, Copenhagen, Denmark, May 2017, pp. 1040-1042. doi:10.18429/JACoW-IPAC2017-MOPVA075

[2] J. M. Köszegi, K. Alomari, J. Knobloch, O. Kugeler, and B. Schmitz, "A Combined Temperature and Magnetic Field Mapping System for SRF Cavities", in *Proc. 9th Int. Particle Accelerator Conf. (IPAC'18)*, Vancouver, Canada, Apr.-May 2018, pp. 1228-1231. doi:10.18429/JACoW-IPAC2018-TUZGBE5

[3] H. Tongu, *et al.*, "Development of nondestructive inspection device for superconducting cavity", in *Proc. 15th Annual Meeting of Particle Accelerator Society of Japan*, Nagaoka, Japan, Aug 2018, pp. 460-463.